N-alkanes as Biomarkers for Latest Pleistocene and Holocene Precipitation in Cores from Tulare Lake, CA, U.S.A.

By

Jeremiah B. Reagan

A Thesis Submitted to the Department of Geology

California State University Bakersfield

In Partial Fulfillment for the Degree of Masters of Science in Geology

Spring 2015

N-alkanes as Biomarkers for Latest Pleistocene and Holocene Precipitation in Cores from Tulare Lake, CA, U.S.A.

By

Jeremiah B. Reagan

This thesis or project has been accepted on behalf of the Department of Geology by their supervisory committee:

Robert Negrini

Committee Chair

Roy LaFever

Dirk Baron

Acknowledgements

Funding provided by the National Science Foundation's Centers of Research Excellence in Science and Technology (CREST) program.

Isotope analysis provided by the Florida International University Stable Isotope Lab.

Phytolith data provided by Kelsey Padilla.

Special thanks to Anna Jacobson and Brandon Pratt for advice and direction to resources on the interpretation of extreme ^{13}C depletion in C3 plants.

Finally, sincere thanks to my advisor Robert Negrini for helping find such an engaging project, and to Roy Lafever for acting as a second advisor and giving me a crash course in organic chemistry.

Abstract

With California suffering from one of the worst droughts on record, accurate models for paleohydrology are in high demand. Understanding the lake level histories of terminal lakes and their connection to Sierran runoff is an important step toward such models. Relative abundance and $\delta^{13}C$ measurements of n-alkanes extracted from Tulare Lake sediment cores are used to test previous interpretations of Holocene lake levels. Ratios of key n-alkanes are used to construct the Carbon Preference Index (CPI), P_{aq}, and the C31 index. Both CPI and P_{aq} values are in agreement with previously measured carbon/nitrogen data and indicate a mostly aquatic assemblage with small but steady input from terrestrial runoff over most of the last 20k years. The C31 index, combined with phytolith counts, shows a dominance of grass in the surrounding watershed during a time interval previously interpreted as containing high lake levels. $\delta^{13}C$ measurements reveal a strong depletion in ^{13}C in this interval. Both the increase in grass abundance and depletion of ^{13}C, particularly in the early Holocene, are taken as evidence of increasing precipitation.

Keywords: N-alkanes, Tulare Lake, Geochemistry

Table of Contents

List of Figures

Introduction

The high resiliency of n-alkanes in the sedimentary record, being relatively unaffected by diagenic processes and not easily broken down below temperatures of 100C, has long made them useful biomarkers for paleoecosystems (Meyers and Ishiwatari, 1993; Feakins and Sessions, 2010; Sachse et al., 2012). Their worth to paleoclimatologists was further increased in the late 1990's, when analytical improvements to isotope-ratio mass spectrometry opened the possibility of measuring the stable-isotope composition of individual organic compounds (Sachse et al., 2012). This opened the door to paleoprecipitation studies using δD of n-alkanes, n-acids, and other lipid components derived from the leaf waxes of watershed plants preserved in lake or marine sediments (Liu and Huang, 2005; Tierney et al., 2008; Niedermeyer et al., 2010; Schefuß et al., 2011). This often necessitated correction to account for differences in plant functional type and photosynthetic pathways (C3 vs C4) which would otherwise obscure shifts in meteoric δD with shifts in vegetation type (Chikaraishi and Naraoka, 2003; Bi et al., 2005; Liu et al., 2006; Smith and Freeman, 2006; Hou et al., 2007; Liu and Yang, 2008; McInerney et al., 2011; Garcin et al., 2012; Wang et al., 2013; Feakins et al., 2014). Fortunately, these differences can be detected in the fractionation of carbon isotopes. Figure 1 (Meyers, P. A. & Lallier-Vergès, 1999) shows typical bulk carbon δ^{13}C values of C3 and C4 plants. In addition to this bulk fractionation, the process of n-alkane synthesis generates a further drop in δ^{13}C values by 4-6‰ for C3 plants and 8-10‰ for C4 plants (Collister et al., 1994; Hobbie and Werner, 2004). The more carbon efficient C4 plants are advantaged under conditions of

low atmospheric CO_2 and favor higher aridity than their C3 counterparts (Ehleringer et al., 1997), making such detectable shifts in vegetation a rough proxy for aridity.

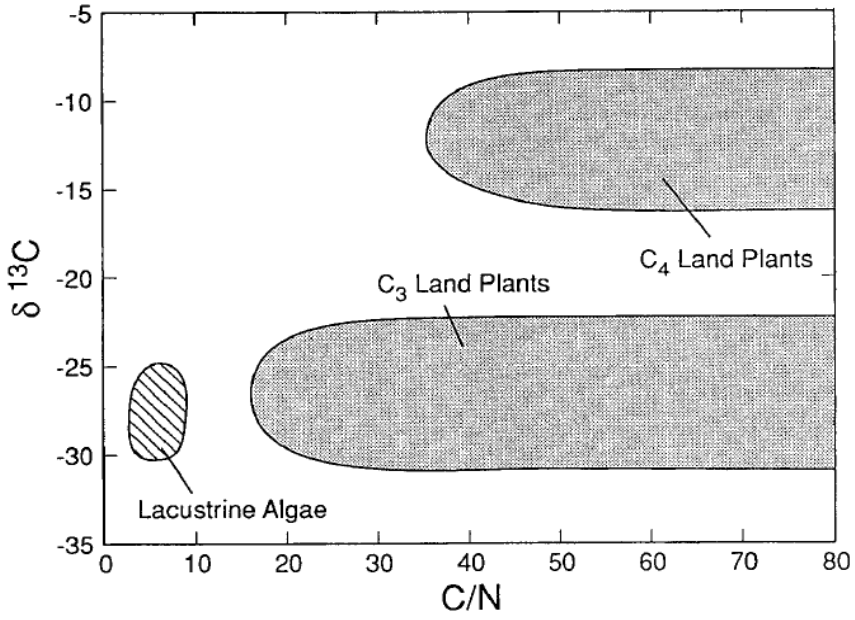

Figure 1: : Range of bulk carbon $\delta^{13}C$ values in C3 and C4 plants (from Meyers, P. A. & Lallier-Vergès, 1999). Lacustrine algae displays similar ranges as C3 terrestrial plants, but tend to contribute more to n-acids and n-alcohols, with n-alkanes dominated by terrestrial input (Eigenbrode, 1999). Production of n-alkanes creates an additional drop of about 4-6‰ and 8-10‰ below bulk values for C3 and C4 plants respectively (Collister et al., 1994; Hobbie and Werner, 2004).

This paper uses n-alkanes extracted from sediment cores of Tulare Lake, California to test previous interpretations of Holocene lake levels as driven by precipitation (Blunt and Negrini, in press), as opposed to non-climatic phenomena, such as avulsion of source rivers. Relative abundances of individual n-alkanes are used to confirm runoff histories provided by previous proxy data and used in conjunction with grass phytolith counts to examine the dominance of grasses in the surrounding watershed. Finally, n-alkane $\delta^{13}C$ data is used as a proxy for aridity.

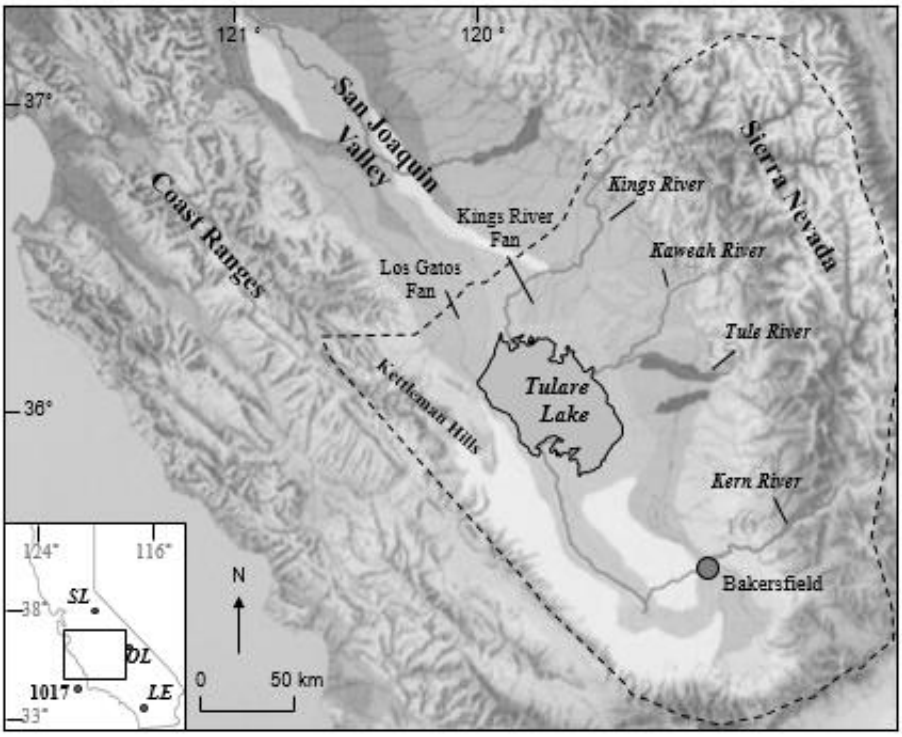

Figure 2: Map of Tulare Lake catchment (Blunt and Negrini, in press).

Regional Setting

Tulare Lake is located in the San Joaquin Valley of central California, between the Coast Ranges and the Sierra Nevada. The basin is fed from the Sierra Nevada by the Kings, Kaweah, Tule, and Kern Rivers. Over the past ~20k years, Tulare Lake has fluctuated by several tens of meters in response to regional climate change and changes in elevation of its alluvial fan-formed spillover sill at the northern end of the lake where the Kings River currently enters the lake basin (Atwater et al., 1986; Negrini et al., 2006). Prior to the agricultural diversion of its tributaries that began in the 1860's and led to its eventual drying by 1899, Tulare Lake was the largest freshwater lake west of the Mississippi and the second largest freshwater lake in the United States based on surface area, with 790 square miles at its highest overflow level of 216 ft. (Preston, 1981; San Joaquin Valley Drainage Program,

1990). Sediment cores were collected in 2005 from the west side of the Tulare Lake Basin, composed primarily of subaqueous silts and clays transported into Tulare Lake by the four major rivers as well as ephemeral streams (Negrini et al., 2006). Mean annual precipitation is only 19.3-21.8 cm (7.6-8.6 in), with 85-92% of rainfall occurring between October and March, and <15% of rainfall occurring from April through September. Low velocity winds typically blow from the northwest and west-northwest with wind speeds of 5-25 kph (3-15 mph) (Preston, 1981). Low precipitation and high temperatures produce evaporation rates of standing water of at least 1m/yr greater than annual precipitation rates, which indicates that Sierran stream runoff is the primary water source for the lake basin (Atwater et al., 1986).

Materials and Methodology

34 samples were collected at 10 cm intervals from refrigerated sediment cores. Samples range from 34 to 440 cm below ground surface, corresponding to ~ 1.8k – 19k calendar years before present, according to the time scale previously established for these cores by (Blunt and Negrini, in press). Samples were ground into a powder with mortar and pestle before being left to dry in a desiccator overnight. Given the low organic content throughout the cores, 10 g was set as a desirable target for minimum post-drying sample mass. However, the depleted condition of the core in several locations from previous experiments led to several samples in the range of 5g - 9g, with a minimum of 4.9g. All post-drying sample masses are listed in table 1 of the appendix.

After weight measurement, samples were transferred into 25 X 150 mm test tubes, which were then filled with a 9:1 CH_2Cl_2 : CH_4O solvent and set to mix overnight to extract hydrocarbons from the sediment. After being allowed to settle by gravity, solvent from each

test tube was transferred to round bottom flasks by use of pipette and glass column, using glass wool as a filter to screen out any accidental transfer of sediment. Remaining sediment was washed into 16 X 125 test tubes and centrifuged with additional solvent. This transfer process was repeated twice in order to maximize the transfer of any extracted hydrocarbon. The extract in the round bottom flasks was then concentrated down to dryness or near dryness with a rotovaporator, rinsed with solvent into 13 X 100 test tubes, and concentrated back down to dryness in a centrivap concentrator. For the purpose of screening out unwanted polar compounds, a miniature chromatography column was constructed for each extract using a pipette, a small amount of glass wool and wash sand, and 1:9 silver-nitrate impregnated silica gel. Bringing the dried extracts back up with a minimal amount of CH_2Cl_2, extracts were placed on the column and eluted through with hexane in two pulses of 1ml each. After concentrating back down to dryness in the centrivap, remaining residue was quantitatively transferred into 2ml HPLC vials and further concentrated and brought up with solvent until a uniform volume of 1ml was reached for all sample extracts.

To measure concentrations of individual n-alkanes, all sample extracts were run in triplicate through a Shimadzu GC-2010 plus GCMS and ramped from 50 C to 300 C at 30 C/min with a hold time of 20 minutes. Individual measurements showing a margin of error > 40% within their triplicate grouping were discarded as outliers. Calibration curves were constructed using standards of 0 mg/ml, 0.01 mg/ml, and 0.1 mg/ml mixtures of C27, C29, C31, C33, and C35 prepared from ultra-pure solids. Minimum detection limits extrapolated from these standards varied by n-alkane, ranging from 0.0025 mg/ml to 0.005 mg/ml. Testing and trouble shooting of the extraction methodology described above was conducted by doping blank test samples of wash sand and Akadama potting soil with the previously

mentioned standard mixtures. With external standards for the other C20 – C36 n-alkanes unavailable, their calibration curves were copied or blended from the next closest n-alkane (details on this process are listed in table 4 of the appendix). The relatively miniscule differences between calibration curves of the standardized n-alkanes suggests this substitution can be made with little risk of additional error.

After GCMS analysis, all sample extracts were packaged and shipped to Florida International University for $\delta^{13}C$ analysis. Low concentrations of target n-alkanes required concentration of sample extracts down to 200 ng/μl. Extracts were then run with a ramp rate of 6 C/min, from 60 C to 300 C, with a hold time of 10 minutes.

Results

Our GCMS method was able to consistently detect concentrations of n-alkanes in all 34 sample (Figures 3 and 4). Furthermore, almost every sample contained detectable amounts of all 17 target n-alkanes with exceptions consisting of 5 samples lacking a single target each. Average σ within original measurement triplicates was 0.484 μg/ml (0.056 μg/g. After filtering of outliers as described in the previous section, this dropped to 0.113 μg/ml (0.014 μg/g). Concentrations of target n-alkanes are tightly clustered, and generally rise and fall as a group, with C24 showing a single surge in dominance at 11.5k years, and C27 and C29 showing similar behavior at 13.8k, 15k, and 17.3k years. C36 remains the most frequently dominant through the time frame, with a large break out around 17.6k years.

Though measurable, these concentrations were low enough to create difficulty in producing reliable isotopic measurements. Only 14 of 34 samples yielded partial carbon data

(Figure 5), with C34 – C36 cut off completely. Most values fall between -25‰ and -35‰, with a large dip from 7k to 11k years ago. This dip is most pronounced in C31, resulting in values down to -37‰.

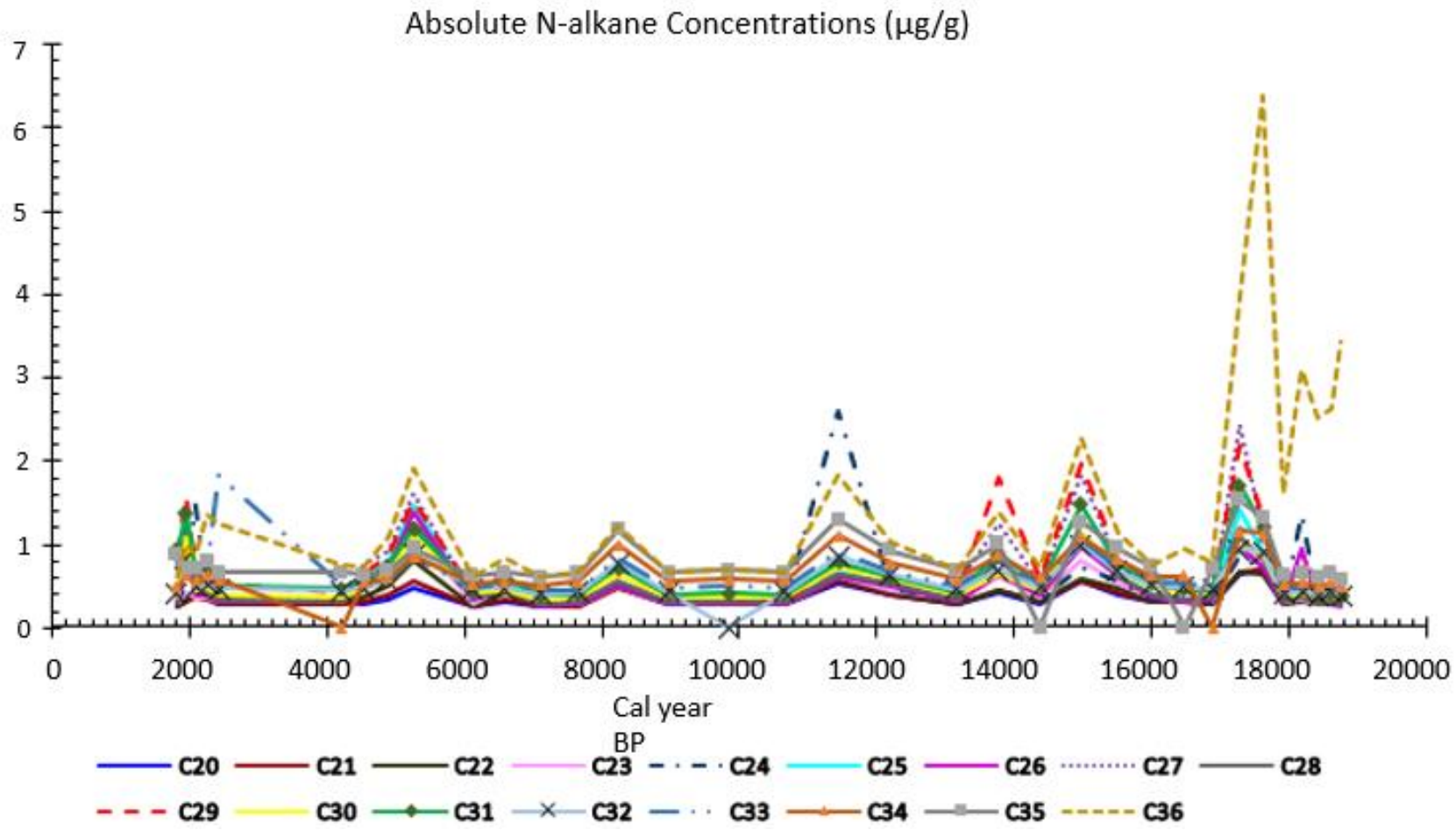

Figure 3: N-alkane concentrations. Table of values is available in the appendix.

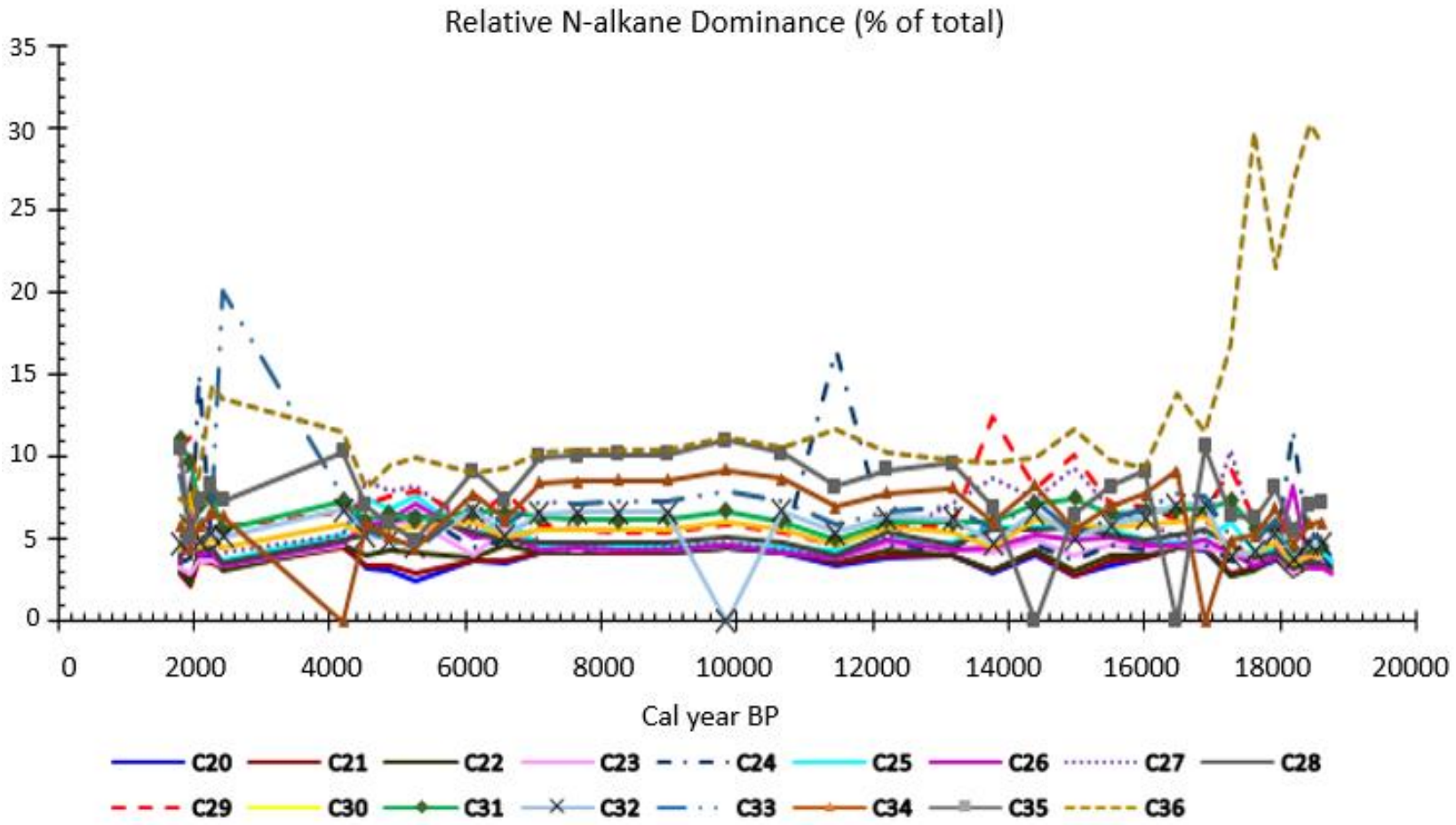

Figure 4: Relative Dominance of measured n-alkanes. Table of values is available in the appendix.

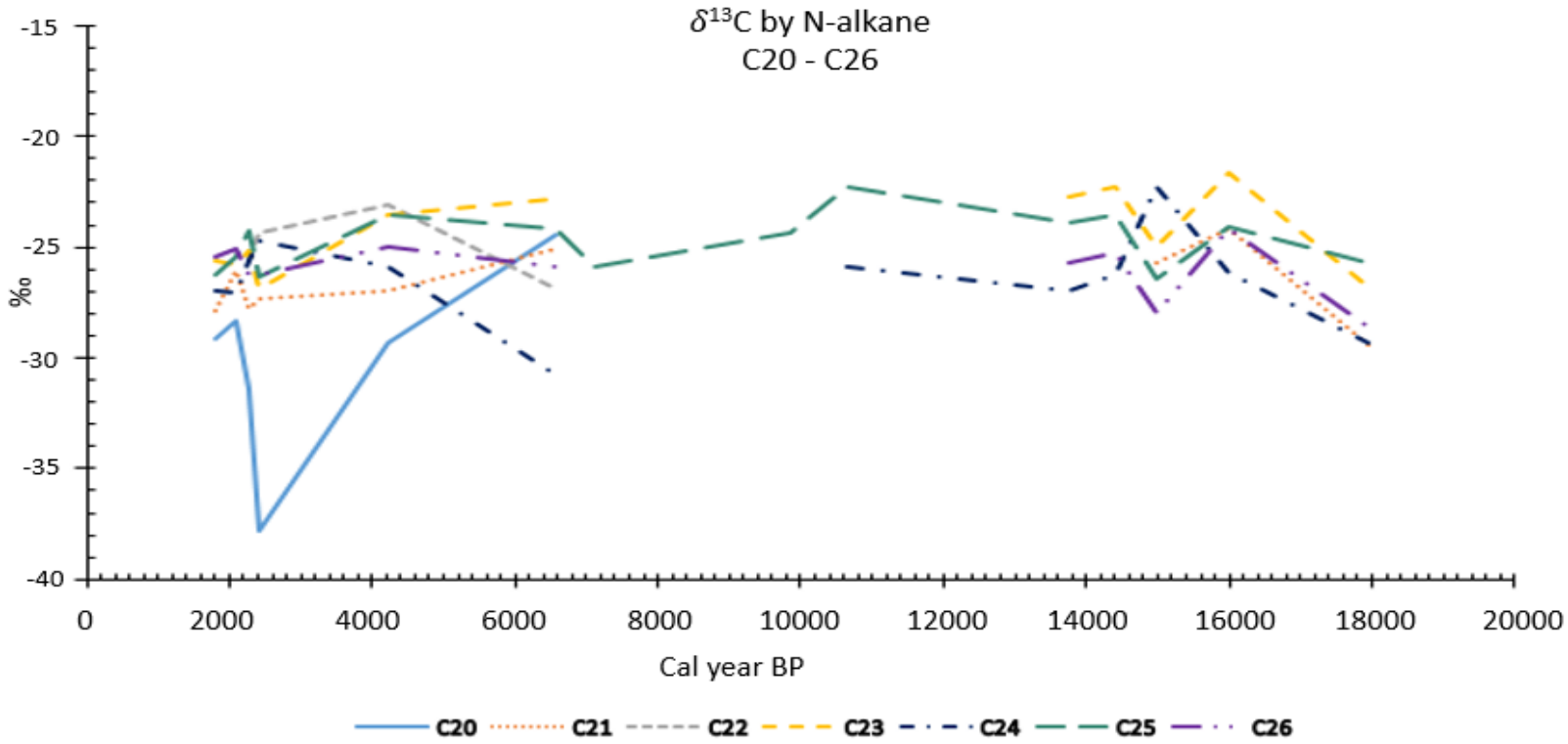

Figure 5a: N-alkane specific carbon isotope data.

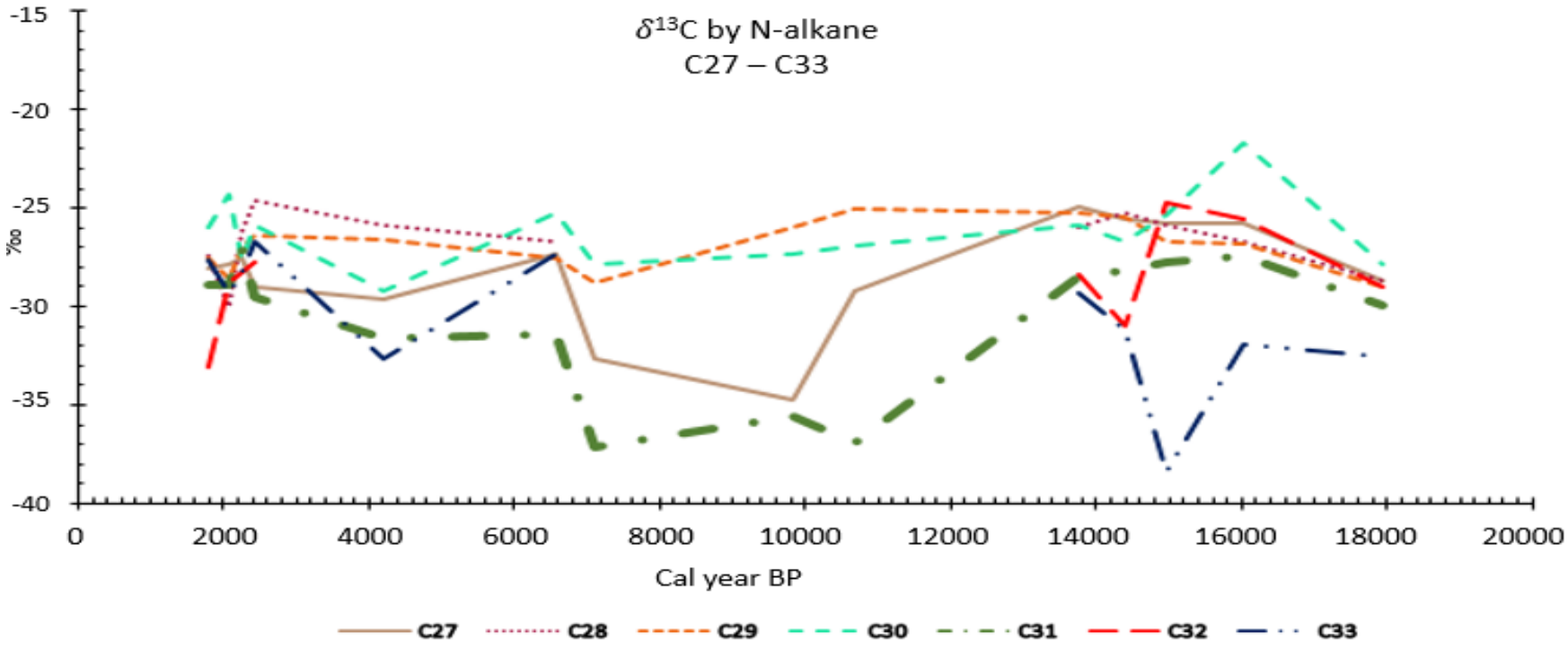

Figure 5b: N-alkane specific carbon isotope data

Discussion

Out of the n-alkane concentration data, three specific ratios were identified as useful paleoclimate indicators for comparison with previously measured proxies.

The Carbon Preference Index (CPI) is a ratio of odd to even n-alkane concentrations given by [Σodd(C21-33) + Σodd(C23-35)]/(2Σeven(C22-34)). Elevated CPI levels (>1) are generally associated with increased input from terrestrial plants, which tend toward an average of ~10.6 when sampled directly (Bush and McInerney, 2013). Serving a similar purpose to the CPI, the aqueous proxy P_{aq} (Ficken et al., 2000) estimates the relative contribution of aquatic vs terrestrial plants and is given by (C23+C25)/(C23+C25+C29+C31). Floating/submerged plants average a direct value of 0.69, with emergent plants at 0.25, and terrestrial plants down at 0.09. As expected, these two measurements display a negative relationship with one another. Increases in CPI are accompanied by decreases in P_{aq}, reflecting an increase in terrestrial input, and vice versa (Figure 6).

P_{aq} values remain heavily weighted towards the aquatic end of the spectrum. Though CPI values do slightly exceed the terrestrial threshold of 1, they are far from the average value of 10.61 found in terrestrial plants. This would suggest a small, steady terrestrial input into a largely aquatic dominated system for most of the past 20k year, with an erratic increase in terrestrial runoff from 4k to 2k years ago. This supports the previously collected C/N data (Figure 6), where a value of 5 serves as a similar terrestrial threshold to that of the CPI. C/N values remain close to this threshold (<10) and display relatively flat behavior over the last

18k to 6k years, indicating a mostly aquatic system with small but significant terrestrial input. This is followed by periodic spikes of increasing magnitude, indicating sudden surges of terrestrial input over the last 6k years.

The third selected indicator is the relative abundance of C31 vs C27 and C29, hereon referred to as the C31 index. Woody angiosperms such as trees and shrubs show a preference for C27 and C29, while grasses produce higher levels of C31 (Meyers and Ishiwatari, 1993). As all three n-alkanes are produced in large amount by all terrestrial plants, this index should only be used for identifying qualitative trends in dominance of grasses vs woody angiosperms (Bush and McInerney, 2013). C31 index results are shown in figure 7, alongside grass phytolith counts and clay% data.

Using clay% as a proxy for lake depth, (Blunt and Negrini, in press) note the similarity in behavior to Pacific sea surface temperature records from an ocean core off the coast of central California (Seki et al., 2002). This is interpreted to suggest that Tulare Lake levels respond directly to SST driven precipitation changes in the Sierra Nevada as opposed to possible alternatives involving migration of the source rivers into and out of the drainage. The C31 index and phytolith counts are further support for lake-level changes driven by climate change, particularly with respect to the high lake level interval centered on 10k years ago. This interval shows an explosive growth in vegetation, which would be well explained by an increase in precipitation.

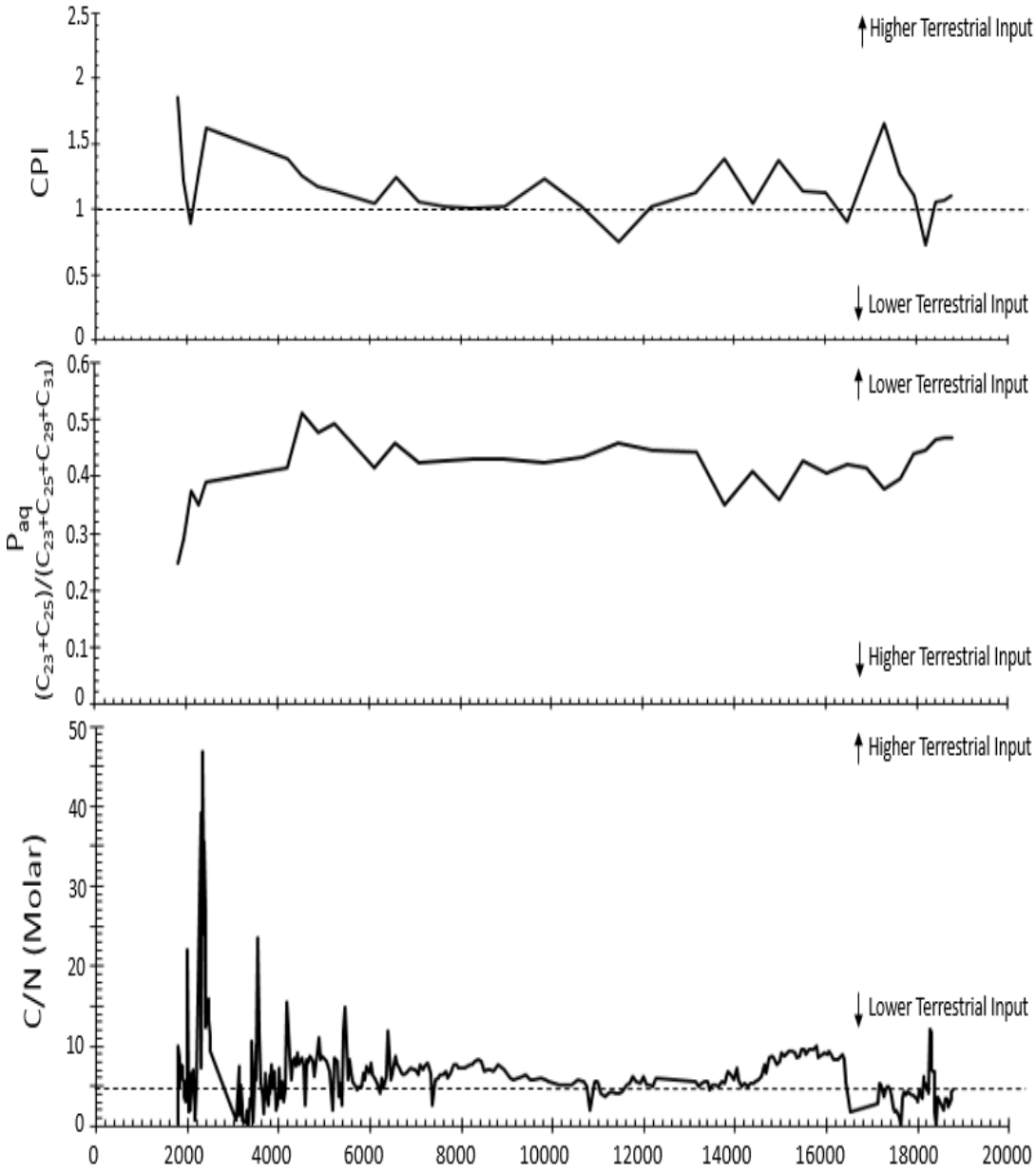

Figure 6: Terrestrial input history of Tulare Lake given by Carbon Preference Index, P_{aq}, and molar Carbon/Nitrogen ratios. Dashed lines indicate thresholds of significant terrestrial input. Average P_{aq} values for directly sampled plants are 0.09 for terrestrial plants, 0.25 for emergent plants, and 0.69 for floating/submerged plants.

Almost all measured $\delta^{13}C$ values fall between -25‰ and -35‰, well within the range of C3 vegetation (Figure 1), suggesting little or no C4 contribution. As C3 and C4 plants are preferentially adapted to wet and arid environments respectively (Ehleringer et al., 1997), this C3 dominance over the past 20k years reflects an environment that is relatively wet, or at the very least, never arid enough to trigger a shift in plant functional groups. C31 displays particularly negative behavior in comparison to other n-alkanes. Given the previously mentioned dominance of grass, it can be safely assumed that this C31 is almost entirely reflective of the behavior of grass alone. In this light, the severe negative behavior of C31 is unsurprising. Owing to a lack of summer growing season, California has been historically deficient in C4 grasses (Teeri and Stowe, 1976). As previously mentioned, n-alkanes show an increased drop in $\delta^{13}C$ values relative to bulk carbon values, with a difference of 4-6‰ in C3 plants, and 8-10‰ in C4 plants. There is a possible extreme case in which this large drop for C4 plants, applied to the bottom end of the C4 spectrum (Figure 1) could result in overlap with the top of the C3 spectrum. However, Conte et al., 2003 have shown that differences between C3 and C4 plants in the carbon discrimination of n-alkane production seem to disappear in a grassland environment. Instead, C4 grasses show the same 4-6‰ drop of C3 grasses. Thus, the extreme case of overlap is highly unlikely.

Although there are no apparent changes between plant functional groups there is still significant shift within the C3 range. For example, there is an especially extreme dip in $\delta^{13}C$ values (down to -37) during the grassy early Holocene high stand from 7k-11k years ago. This in itself tells us something about available moisture. The mechanics of carbon discrimination in photosynthesis, in addition to being driven by enzymatic processes, are

partially driven by stomatal respiration and diffusion across stomatal pores and boundary layers (Farquhar, 1989). Under more arid conditions, plants keep their stomata closed more often to reduce water loss. The adaptations that allow C4 and CAMS plants to thrive in arid environments directly relate to their ability to photosynthesize while keeping their stomata closed for longer periods of time. Likewise, drops in $\delta^{13}C$ within the same or similar species of plants are associated with increased respiration, suggesting more available moisture.

There is a possibility that the severity of the dip could represent a canopy effect of C3 grasses growing in shade (Kohn, 2010), though given the lack of input from trees relative to grasses as shown by the C31 index (Figure 7), such undergrowth would have to have been preferentially transported in from the margins of the basin, or else be indicative of persistently overcast conditions. Whether this dip in the signal is due to an explosive growth of shade providing trees, overcast skies, or increased respiration of existing C3 grasses, all would be evidence of increased precipitation coinciding with both an explosive growth of grass phytoliths, and the high lake levels of the early Holocene.

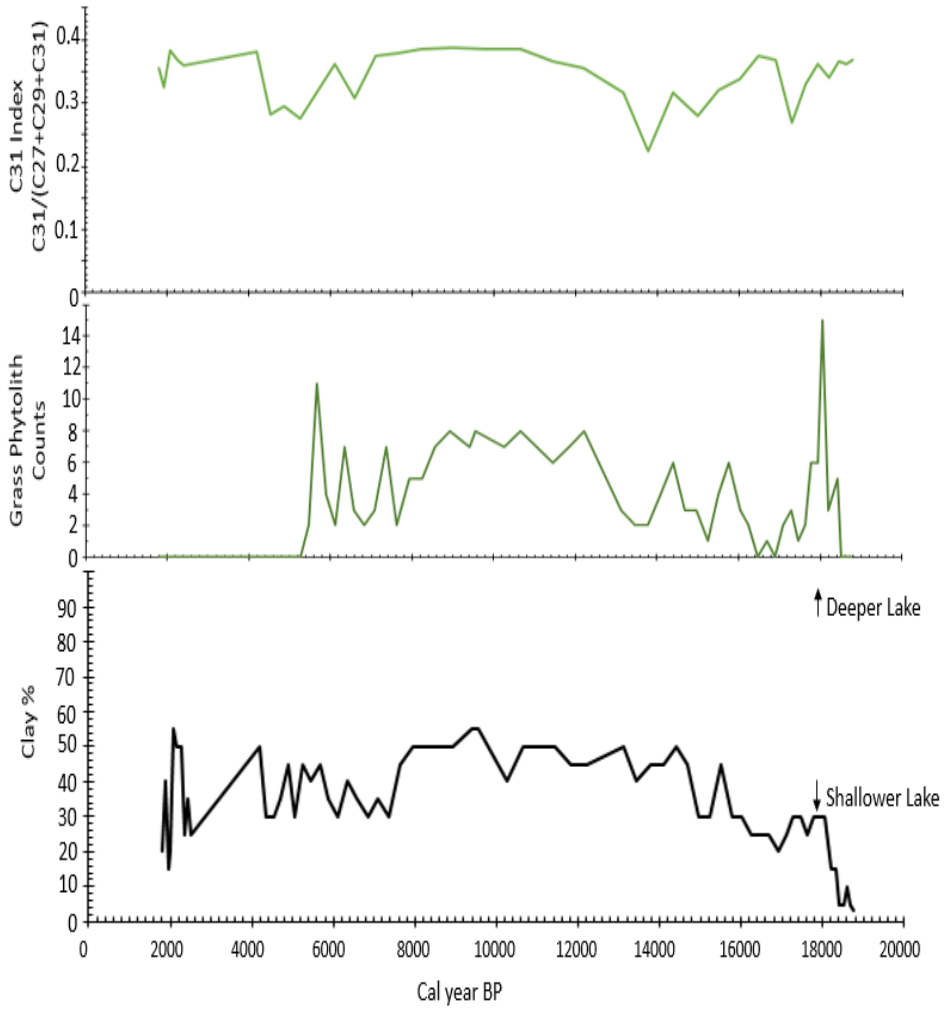

Figure 7: C31 index, grass phytoliths, and clay% (Blunt and Negrini, in press). The C31 index lacks a defined threshold value for determining grass vs woody angiosperm contribution quantitatively. Instead, it reflects shifts in trends over time. However, the matchup between grass phytolith counts in the core and the rise and fall of relative C31 abundance supports the interpretation of an overall dominance of grasses in the surrounding watershed during this lake level highstand.

Conclusions

The increased abundance of grass indicated by n-alkane C31 and grass phytolith counts during the latest Pleistocene/early Holocene highstand in Tulare Lake supports the previous interpretation (Blunt and Negrini, in press) of increasing regional precipitation as the cause for high lake levels at this time. This is further supported by the extreme negative swing in C31 δ^{13}C values in this same time period, indicating increased carbon discrimination across stomatal boundaries as grasses keep their stomata open more often in an environment where moisture is more abundant. The extremity of the δ^{13}C swing also leaves open the possibility of increased shade as a partial factor, whether due to overcast skies or a canopy effect from other vegetation.

GCMS analysis of relative n-alkane abundances proved an effective and relatively straightforward and inexpensive means of tracking grass abundance, as well as providing independent confirmation of C/N data and similar terrestrial runoff proxies through the use of CPI and P_{aq} values, even in a lake with very low organic carbon and poor pollen preservation (Medina, 2015). Though low concentrations led to gaps in the δ^{13}C data, this problem could be avoided by simply scaling up the initial sample mass. Unfortunately, the nearly exhausted condition of the available cores limited the amount of sample material available for this project. With the benefit of higher n-alkane concentrations, future efforts could include additional δD analysis of individual n-alkanes, allowing for more direct investigation of paleoprecipitation once corrected for vegetation effects with δ^{13}C data.

Appendix

Table 1: List of samples with depth below ground surface, age based on timescale from (Blunt and Negrini, in review), and post-drying sample mass.

Sample ID	Depth (cm bgs)	Age (calyr bp)	Sample Mass (g)
1-040	34	1802	11.46
1-050	44	1942	10.42
1-060	54	2093	10.04
1-070	65	2256	9.43
1-080	74	2431	10.05
2-010	147	4210	9.87
2-020	157	4528	10.46
2-030	167	4880	10.17
2-040	177	5260	7.13
2-060	197	6110	10.48
2-070	207	6586	10.05
2-080	217	7098	10.63
2-090	227	7650	10.03
2-100	237	8245	5.54
2-110	247	8975	9.84
2-120	257	9841	9.53
2-130	267	10667	9.82
2-140	277	11454	5.04
2-150	287	12202	7.08
3-010	300	13166	9.50
3-020	310	13774	6.88
3-030	320	14393	9.31
3-040	330	14972	5.45
3-050	340	15513	6.90

3-060	350	16014	8.88
3-070	360	16476	8.93
3-080	370	16898	9.25
3-090	380	17282	4.86
3-100	390	17626	4.99
3-110	400	17931	10.61
3-120	410	18197	10.18
3-130	420	18424	11.16
3-140	430	18611	10.21
3-150	440	18759	11.28

Table 2: Absolute n-alkane concentrations by mass.

Age (calyr bp)	C20 µg/g	C21 µg/g	C22 µg/g	C23 µg/g	C24 µg/g	C25 µg/g	C26 µg/g	C27 µg/g	C28 µg/g	C29 µg/g	C30 µg/g	C31 µg/g	C32 µg/g	C33 µg/g	C34 µg/g	C35 µg/g	C36 µg/g
1802	0.2595	0.24897	0.26307	0.27021	0.29337	0.3222	0.30073	0.79843	0.32805	0.88773	0.36133	0.93048	0.39762	0.74753	0.48999	0.88714	0.62397
1942	0.34101	0.31252	0.33468	0.41458	0.55667	0.8035	0.92196	1.27927	1.19089	1.58797	1.0943	1.37716	0.83292	0.77895	0.62694	0.71641	1.01223
2093	0.39058	0.37094	0.45886	0.36845	1.47971	0.4367	0.40346	0.47145	0.42127	0.65272	0.44375	0.6992	0.47936	0.58765	0.56799	0.72145	0.87109
2256	0.38319	0.32995	0.38336	0.35502	0.39857	0.394	0.39772	0.55108	0.41783	0.6748	0.47298	0.71651	0.51215	0.69671	0.61749	0.78296	1.35777
2431	0.32714	0.29405	0.28783	0.30948	0.31705	0.3407	0.3026	0.37413	0.32958	0.51973	0.402	0.50149	0.46748	1.82753	0.58305	0.66517	1.23704
4210	0.31016	0.29383	0.3051	0.30357	0.30696	0.3408	0.31216	0.33907	0.32488	0.4306	0.37901	0.47281	0.44069	0.49392	0	0.66565	0.74887
4528	0.29495	0.31355	0.36143	0.57842	0.47951	0.667	0.51812	0.76482	0.4757	0.63958	0.48156	0.55322	0.47115	0.50159	0.53375	0.63671	0.73501
4880	0.34938	0.38235	0.50329	0.68831	0.66205	0.7847	0.70471	0.91052	0.69459	0.8725	0.63558	0.74435	0.56146	0.56113	0.5927	0.67519	1.07842
5260	0.49021	0.55625	0.80643	1.17643	1.27854	1.4671	1.38191	1.60168	1.25093	1.52922	1.10906	1.19121	0.88291	0.84619	0.85353	0.95044	1.91023
6110	0.25608	0.25813	0.2624	0.27881	0.30667	0.3456	0.35017	0.38041	0.36683	0.4243	0.4096	0.45515	0.46565	0.48855	0.52667	0.62309	0.62117
6586	0.31857	0.32757	0.41954	0.51804	0.44254	0.572	0.47276	0.64146	0.44143	0.69386	0.45368	0.59403	0.47027	0.53466	0.55657	0.66318	0.84372
7098	0.25201	0.25474	0.25862	0.27128	0.26551	0.2777	0.26656	0.29225	0.29155	0.35842	0.33861	0.38884	0.40112	0.44544	0.51838	0.61336	0.62892
7650	0.26667	0.26727	0.27281	0.27918	0.281	0.2907	0.28804	0.2991	0.30948	0.36225	0.36384	0.40279	0.428	0.46162	0.54911	0.65005	0.67194
8245	0.49147	0.48978	0.50091	0.50176	0.52614	0.5193	0.50088	0.50842	0.54797	0.63357	0.64916	0.71661	0.76739	0.83845	0.99899	1.17509	1.20908
8975	0.27334	0.27355	0.27426	0.28087	0.28687	0.2942	0.28088	0.2876	0.30741	0.35535	0.3648	0.4065	0.43203	0.47358	0.5593	0.66057	0.6807
9841	0.28428	0.27991	0.28275	0.28843	0.29004	0.2936	0.28786	0.29556	0.31649	0.36726	0.37707	0.41658	0	0.49108	0.57643	0.6852	0.69558
10667	0.27533	0.27982	0.27645	0.28263	0.28313	0.2911	0.27514	0.28445	0.30794	0.35031	0.3654	0.39647	0.43414	0.47318	0.56111	0.66497	0.68405
11454	0.54372	0.56061	0.58989	0.62023	2.5977	0.673	0.60139	0.63558	0.63264	0.73677	0.73606	0.79101	0.85244	0.92857	1.09898	1.29233	1.83743
12202	0.38987	0.39903	0.42882	0.46128	0.4729	0.5006	0.49153	0.51883	0.54197	0.58804	0.57966	0.6097	0.63191	0.67655	0.78011	0.9209	1.02471
13166	0.28369	0.28851	0.29194	0.32676	0.30773	0.345	0.31412	0.51439	0.33613	0.41404	0.38527	0.42982	0.44913	0.49632	0.58111	0.68579	0.70005
13774	0.42392	0.44565	0.45627	0.60381	0.86683	0.8345	0.63913	1.26211	0.80781	1.7907	0.65451	0.88469	0.68625	0.79603	0.86413	1.00436	1.39368
14393	0.29662	0.30228	0.3159	0.35796	0.34042	0.4151	0.38397	0.541	0.4111	0.58897	0.45357	0.5213	0.48344	0.53061	0.60022	0	0.72085

14972	0.5492	0.55489	0.59476	0.79864	0.73723	1.1447	0.98355	1.82508	1.12106	1.97737	1.14797	1.47278	0.99427	1.0685	1.09647	1.27095	2.2832
15513	0.39922	0.42284	0.46395	0.5437	0.54623	0.6478	0.60158	0.78647	0.61914	0.83961	0.66547	0.76425	0.68017	0.72464	0.82037	0.95024	1.13781
16014	0.30765	0.31243	0.32102	0.35549	0.35036	0.3961	0.3704	0.48836	0.40405	0.56456	0.47155	0.53904	0.5129	0.55443	0.62209	0.73649	0.74827
16476	0.30304	0.3088	0.30759	0.31259	0.32436	0.3293	0.31661	0.34714	0.35214	0.41732	0.41235	0.45875	0.48093	0.53005	0.61844	0	0.94212
16898	0.28874	0.29512	0.29619	0.30446	0.30846	0.3302	0.32769	0.36216	0.37516	0.43027	0.42033	0.46018	0.47499	0.50991	0	0.70703	0.7725
17282	0.65485	0.67717	0.66822	0.96282	0.87462	1.4098	0.97936	2.44856	1.07495	2.19342	0.98446	1.71331	0.93502	1.2037	1.15651	1.52675	3.94371
17626	0.68931	0.69212	0.65104	0.74703	0.69996	0.9299	0.73185	1.15431	0.83382	1.33267	0.90255	1.21844	0.90917	1.03474	1.12644	1.32866	6.375
17931	0.27584	0.28901	0.28644	0.31819	0.29525	0.3228	0.28628	0.33773	0.30999	0.39962	0.36266	0.41847	0.40416	0.46748	0.52074	0.61499	1.61553
18197	0.41176	0.34599	0.31338	0.34619	1.34967	0.4359	0.95034	0.43779	0.37682	0.49411	0.41677	0.47839	0.4395	0.48379	0.54464	0.6444	3.09717
18424	0.37965	0.31935	0.28778	0.29584	0.3384	0.3367	0.27286	0.29659	0.29313	0.35245	0.34116	0.37485	0.3874	0.43011	0.49334	0.5908	2.52278
18611	0.4272	0.36211	0.32022	0.33644	0.36323	0.3698	0.29528	0.32811	0.3162	0.3921	0.3638	0.40793	0.42375	0.46621	0.54157	0.64349	2.61767
18759	0.32619	0.33305	0.29728	0.32169	0.30087	0.3461	0.26713	0.30378	0.29634	0.36732	0.33446	0.39125	0.38696	0.42376	0.49154	0.58023	3.44086

Table 3: Relative n-alkane dominance. Out of 100%

Age (calyr bp)	C20	C21	C22	C23	C24	C25	C26	C27	C28	C29	C30	C31	C32	C33	C34	C35	C36
1802	3.09	2.96	3.13	3.21	3.49	3.83	3.58	9.49	3.90	10.56	4.30	11.06	4.73	8.89	5.83	10.55	7.42
1942	2.40	2.20	2.36	2.92	3.93	5.67	6.50	9.02	8.40	11.20	7.72	9.71	5.87	5.49	4.42	5.05	7.14
2093	3.98	3.78	4.67	3.75	15.06	4.45	4.11	4.80	4.29	6.64	4.52	7.12	4.88	5.98	5.78	7.34	8.87
2256	4.06	3.49	4.06	3.76	4.22	4.17	4.21	5.84	4.43	7.15	5.01	7.59	5.42	7.38	6.54	8.29	14.38
2431	3.60	3.24	3.17	3.41	3.49	3.75	3.33	4.12	3.63	5.72	4.42	5.52	5.15	20.11	6.42	7.32	13.61
4210	4.80	4.54	4.72	4.69	4.75	5.27	4.83	5.24	5.02	6.66	5.86	7.31	6.81	7.64	0.00	10.29	11.58
4528	3.27	3.48	4.01	6.42	5.32	7.41	5.75	8.49	5.28	7.10	5.35	6.14	5.23	5.57	5.93	7.07	8.16
4880	3.06	3.35	4.41	6.04	5.81	6.88	6.18	7.99	6.09	7.65	5.57	6.53	4.92	4.92	5.20	5.92	9.46

5260	2.54	2.88	4.18	6.10	6.63	7.61	7.17	8.31	6.49	7.93	5.75	6.18	4.58	4.39	4.43	4.93	9.91
6110	3.76	3.79	3.85	4.09	4.50	5.07	5.13	5.58	5.38	6.22	6.01	6.67	6.83	7.16	7.72	9.14	9.11
6586	3.55	3.65	4.68	5.78	4.94	6.38	5.27	7.16	4.92	7.74	5.06	6.63	5.25	5.96	6.21	7.40	9.41
7098	4.12	4.16	4.22	4.43	4.34	4.54	4.35	4.77	4.76	5.85	5.53	6.35	6.55	7.27	8.47	10.02	10.27
7650	4.14	4.15	4.23	4.33	4.36	4.51	4.47	4.64	4.80	5.62	5.65	6.25	6.64	7.16	8.52	10.09	10.43
8245	4.25	4.23	4.33	4.33	4.55	4.49	4.33	4.39	4.73	5.47	5.61	6.19	6.63	7.24	8.63	10.15	10.45
8975	4.21	4.21	4.22	4.33	4.42	4.53	4.33	4.43	4.74	5.47	5.62	6.26	6.65	7.29	8.62	10.18	10.49
9841	4.56	4.49	4.54	4.63	4.66	4.71	4.62	4.75	5.08	5.90	6.05	6.69	0.00	7.88	9.26	11.00	11.17
10667	4.25	4.31	4.26	4.36	4.37	4.49	4.24	4.39	4.75	5.40	5.63	6.11	6.69	7.30	8.65	10.25	10.55
11454	3.46	3.56	3.75	3.94	16.52	4.28	3.82	4.04	4.02	4.68	4.68	5.03	5.42	5.90	6.99	8.22	11.68
12202	3.89	3.98	4.28	4.61	4.72	5.00	4.91	5.18	5.41	5.87	5.79	6.09	6.31	6.75	7.79	9.19	10.23
13166	3.97	4.04	4.08	4.57	4.30	4.82	4.39	7.19	4.70	5.79	5.39	6.01	6.28	6.94	8.13	9.59	9.79
13774	2.94	3.09	3.17	4.19	6.01	5.79	4.43	8.76	5.60	12.42	4.54	6.14	4.76	5.52	5.99	6.97	9.67
14393	4.08	4.16	4.35	4.93	4.69	5.72	5.29	7.45	5.66	8.11	6.24	7.18	6.66	7.31	8.26	0.00	9.92
14972	2.80	2.83	3.03	4.07	3.76	5.83	5.01	9.30	5.71	10.08	5.85	7.51	5.07	5.45	5.59	6.48	11.64
15513	3.44	3.64	3.99	4.68	4.70	5.58	5.18	6.77	5.33	7.23	5.73	6.58	5.86	6.24	7.06	8.18	9.80
16014	3.82	3.88	3.99	4.41	4.35	4.92	4.60	6.06	5.02	7.01	5.85	6.69	6.37	6.88	7.72	9.14	9.29
16476	4.48	4.57	4.55	4.62	4.80	4.87	4.68	5.13	5.21	6.17	6.10	6.78	7.11	7.84	9.15	0.00	13.93
16898	4.33	4.43	4.44	4.57	4.63	4.96	4.92	5.44	5.63	6.46	6.31	6.91	7.13	7.65	0.00	10.61	11.59
17282	2.80	2.89	2.85	4.11	3.74	6.02	4.18	10.46	4.59	9.37	4.21	7.32	3.99	5.14	4.94	6.52	16.85
17626	3.23	3.24	3.05	3.50	3.28	4.35	3.43	5.40	3.90	6.24	4.23	5.71	4.26	4.84	5.27	6.22	29.85

17931	3.67	3.84	3.81	4.23	3.92	4.29	3.80	4.49	4.12	5.31	4.82	5.56	5.37	6.21	6.92	8.17	21.47
18197	3.56	2.99	2.71	2.99	11.67	3.77	8.22	3.78	3.26	4.27	3.60	4.14	3.80	4.18	4.71	5.57	26.78
18424	4.57	3.84	3.46	3.56	4.07	4.05	3.28	3.57	3.53	4.24	4.10	4.51	4.66	5.17	5.93	7.11	30.35
18611	4.76	4.03	3.57	3.75	4.05	4.12	3.29	3.66	3.52	4.37	4.05	4.55	4.72	5.19	6.03	7.17	29.17
18759	3.54	3.62	3.23	3.49	3.27	3.76	2.90	3.30	3.22	3.99	3.63	4.25	4.20	4.60	5.34	6.30	37.36

Table 4: Calibration curve equations. The following table contains slope and intercept values for the linear equations of the form $y=mx*10^{7}-b$ where x is the peak area detected by the GCMS for an individual n-alkane, and y is the concentration in mg/ml. Marked equations were generated automatically by the software using premixed standards of selected n-alkanes, while others were generated by borrowing or averaging adjacent values.

N-alkane	m	b	Standard?
C20	3.241234	85079.26	
C21	3.241234	85079.26	
C22	3.241234	85079.26	
C23	3.241234	85079.26	
C24	3.241234	85079.26	
C25	3.241234	85079.26	
C26	3.241234	85079.26	
C27	3.241234	85079.26	Y
C28	3.214073	95012.63	
C29	3.186912	104946.2	Y
C30	3.068369	108783.8	
C31	2.949826	112621.4	Y
C32	3.0460115	128840.65	
C33	3.142197	145059.9	Y
C34	2.9052115	159164.9	
C35	2.668226	173269.9	Y
C36	2.668226	173269.9	

References

Atwater, B., Adam, D., Bradbury, P., Forester, R., Mark, R., Lettis, W., Fisher, R., Gobalet, K., Robinson, S., 1986. A fan dam for Tulare Lake, California, and implications for the Wisconsin glacial history of the Sierra Nevada. Geol. Soc. Am. Bull. 97, 97–109.

Bi, X., Sheng, G., Liu, X., Li, C., Fu, J., 2005. Molecular and carbon and hydrogen isotopic composition of n-alkanes in plant leaf waxes. Org. Geochem. 36, 1405–1417. doi:10.1016/j.orggeochem.2005.06.001

Blunt, A., Negrini, R.M., n.d. Latest Pleistocene through Holocene Lake Levels from the TL05-4 Cores, Tulare Lake, CA, USA. California State University Bakersfield.

Bush, R.T., McInerney, F. a., 2013. Leaf wax n-alkane distributions in and across modern plants: Implications for paleoecology and chemotaxonomy. Geochim. Cosmochim. Acta 117, 161–179. doi:10.1016/j.gca.2013.04.016

Chikaraishi, Y., Naraoka, H., 2003. Compound-specific ??D-??13C analyses of n-alkanes extracted from terrestrial and aquatic plants. Phytochemistry 63, 361–371. doi:10.1016/S0031-9422(02)00749-5

Collister, J.W., Rieley, G., Stern, B., Eglinton, G., Fry, B., 1994. Compound-specific δ 13C analyses of leaf lipids from plants with differing carbon dioxide metabolisms. Org. Geochem. doi:10.1016/0146-6380(94)90008-6

Conte, M.H., Weber, J.C., Carlson, P.J., Flanagan, L.B., 2003. Molecular and carbon isotopic composition of leaf wax in vegetation and aerosols in a northern prairie ecosystem. Oecologia 135, 67–77. doi:10.1007/s00442-002-1157-4

Ehleringer, J.R., Cerling, T.E., Helliker, B.R., 1997. C 4 photosynthesis, atmospheric CO 2 , and climate. Oecologia 112, 285–299. doi:10.1007/s004420050311

Eigenbrode, J., 1999. Sedimentological, Carbon-Isotopic, and Molecular Records of Late Holocene CLimate in the Sediments of Soda Lake, Carrizo Plain, California. Indiana University.

Farquhar, G., 1989. Carbon Isotope Discrimination And Photosynthesis. Annu. Rev. Plant Physiol. Plant Mol. Biol. 40, 503–537. doi:10.1146/annurev.arplant.40.1.503

Feakins, S.J., Kirby, M.E., Cheetham, M.I., Ibarra, Y., Zimmerman, S.R.H., 2014. Fluctuation in leaf wax D/H ratio from a southern California lake records significant variability in isotopes in precipitation during the late Holocene. Org. Geochem. 66, 48–59. doi:10.1016/j.orggeochem.2013.10.015

Feakins, S.J., Sessions, A.L., 2010. Controls on the D/H ratios of plant leaf waxes in an arid ecosystem. Geochim. Cosmochim. Acta 74, 2128–2141. doi:10.1016/j.gca.2010.01.016

Ficken, K.J., Li, B., Swain, D.L., Eglinton, G., 2000. An n -alkane proxy for the sedimentary input of submerged / ¯ oating freshwater aquatic macrophytes. Org. Geochem. 31, 745–749.

Garcin, Y., Schwab, V.F., Gleixner, G., Kahmen, A., Todou, G., Séné, O., Onana, J.M., Achoundong, G., Sachse, D., 2012. Hydrogen isotope ratios of lacustrine sedimentary n-alkanes as proxies of tropical African hydrology: Insights from a calibration transect across Cameroon. Geochim. Cosmochim. Acta 79, 106–126. doi:10.1016/j.gca.2011.11.039

Hobbie, E. a, Werner, R. a, 2004. Bulk carbon isotope patterns in C 3 and C 4 plants : a review and synthesis. New Phytol. 161, 371–385. doi:10.1046/j.1469-8137.2004.00970.x

Hou, J., D'Andrea, W.J., MacDonald, D., Huang, Y., 2007. Evidence for water use efficiency as an important factor in determining the δD values of tree leaf waxes. Org. Geochem. 38, 1251–1255. doi:10.1016/j.orggeochem.2007.03.011

Kohn, M.J., 2010. Carbon isotope compositions of terrestrial C3 plants as indicators of (paleo)ecology and (paleo)climate. Proc. Natl. Acad. Sci. U. S. A. 107, 19691–19695. doi:10.1073/pnas.1004933107

Liu, W., Huang, Y., 2005. Compound specific D/H ratios and molecular distributions of higher plant leaf waxes as novel paleoenvironmental indicators in the Chinese Loess Plateau. Org. Geochem. 36, 851–860. doi:10.1016/j.orggeochem.2005.01.006

Liu, W., Yang, H., 2008. Multiple controls for the variability of hydrogen isotopic compositions in higher plant n-alkanes from modern ecosystems. Glob. Chang. Biol. 14, 2166–2177. doi:10.1111/j.1365-2486.2008.01608.x

Liu, W., Yang, H., Li, L., 2006. Hydrogen isotopic compositions of n-alkanes from terrestrial plants correlate with their ecological life forms. Oecologia 150, 330–338. doi:10.1007/s00442-006-0494-0

McInerney, F. a., Helliker, B.R., Freeman, K.H., 2011. Hydrogen isotope ratios of leaf wax n-alkanes in grasses are insensitive to transpiration. Geochim. Cosmochim. Acta 75, 541–554. doi:10.1016/j.gca.2010.10.022

Meyers, P. a., Ishiwatari, R., 1993. Lacustrine organic geochemistry—an overview of indicators of organic matter sources and diagenesis in lake sediments. Org. Geochem. 20, 867–900. doi:10.1016/0146-6380(93)90100-P

Meyers, P. A. & Lallier-Vergès, E., 1999. Lacustrine sedimentary organic matter of Late Quaternary paleoclimates. J. Paleolimnol. 21, 345–372.

Negrini, R.M., Wigand, P.E., Draucker, S., Gobalet, K., Gardner, J.K., Sutton, M.Q., Yohe, R.M., 2006. The Rambla highstand shoreline and the Holocene lake-level history of Tulare Lake, California, USA. Quat. Sci. Rev. 25, 1599–1618. doi:10.1016/j.quascirev.2005.11.014

Niedermeyer, E.M., Schefuß, E., Sessions, A.L., Mulitza, S., Mollenhauer, G., Schulz, M., Wefer, G., 2010. Orbital- and millennial-scale changes in the hydrologic cycle and vegetation in the western African Sahel: Insights from individual plant wax δD and δ13C. Quat. Sci. Rev. 29, 2996–3005. doi:10.1016/j.quascirev.2010.06.039

Preston, W.L., 1981. Vanishing Landscapes: Land and life in the Tulare Lake Basin. University of California Press, Berkeley.

Sachse, D., Billault, I., Bowen, G.J., Chikaraishi, Y., Dawson, T.E., Feakins, S.J., Freeman, K.H., Magill, C.R., McInerney, F. a., van der Meer, M.T.J., Polissar, P., Robins, R.J., Sachs, J.P., Schmidt, H.-L., Sessions,

A.L., White, J.W.C., West, J.B., Kahmen, A., 2012. Molecular Paleohydrology: Interpreting the Hydrogen-Isotopic Composition of Lipid Biomarkers from Photosynthesizing Organisms. Annu. Rev. Earth Planet. Sci. 40, 221–249. doi:10.1146/annurev-earth-042711-105535

San Joaquin Valley Drainage Program: Draft Final Report, 1990. . Sacramento, CA.

Schefuß, E., Kuhlmann, H., Mollenhauer, G., Prange, M., Pätzold, J., 2011. Forcing of wet phases in southeast Africa over the past 17,000 years. Nature 480, 509–512. doi:10.1038/nature10685

Seki, O., Ishiwatari, R., Matsumoto, K., 2002. Millennial climate oscillations in NE Pacific surface waters over the last 82 kyr: New evidence from alkenones. Geophys. Res. Lett. 29, 1–4. doi:10.1029/2002GL015200

Smith, F. a., Freeman, K.H., 2006. Influence of physiology and climate on ??D of leaf wax n-alkanes from C3 and C4 grasses. Geochim. Cosmochim. Acta 70, 1172–1187. doi:10.1016/j.gca.2005.11.006

Teeri, J.A., Stowe, L.G., 1976. Climatic patterns and the distribution of C4 grasses in North America. Oecologia 23, 1–12. doi:10.1007/BF00351210

Tierney, J.E., Russell, J.M., Huang, Y., Damsté, J.S.S., Hopmans, E.C., Cohen, A.S., 2008. Northern hemisphere controls on tropical southeast African climate during the past 60,000 years. Science 322, 252–255. doi:10.1126/science.1160485

Wang, Y. V., Larsen, T., Leduc, G., Andersen, N., Blanz, T., Schneider, R.R., 2013. What does leaf wax δD from a mixed C3/C4 vegetation region tell us? Geochim. Cosmochim. Acta 111, 128–139. doi:10.1016/j.gca.2012.10.016